VIP Heterogeneous Catalysis

DOI: 10.1002/anie.200902800

Fast Prediction of Selectivity in Heterogeneous Catalysis from Extended Brønsted–Evans–Polanyi Relations: A Theoretical Insight**

David Loffreda, Françoise Delbecq, Fabienne Vigné, and Philippe Sautet*

Understanding kinetics and reaction mechanisms is a major challenge in catalysis. Theoretical chemistry can offer a unique input by identifying the transition states and the associated activation barriers for elementary reaction steps. However, their determination requires intensive quantum chemical computations, and hence the theoretical exploration of complex catalytic reaction networks at solid surfaces remains a tremendous challenge. Simpler methods to rapidly determine activation energy barriers are therefore needed for a preliminary screening.

The parametrization of reactive force fields is a fast and simplified solution to evaluate the total electronic energy and forces. However, the accurate treatment of molecular interactions at metallic surfaces remains difficult. Another approach is by using Brønsted–Evans–Polanyi (BEP) relations, which classically link kinetics (activation barriers) with thermodynamics (reaction enthalpies).[1] These relations, examined in recent density functional theory (DFT) studies on the dissociation of small molecules over transition-metal surfaces,[2–6] are established for a given reactant and an elementary step by varying the nature of the catalyst. In these studies, the activation energy barrier is plotted against either the reaction energy or the stability of the final dissociated state. However, this relation has not been examined for multifunctional reactants, where the chemical nature of the atoms neighboring the reactive centers changes. This would be truly valuable for fine chemistry reactions, particularly in regard to selectivity issues.

The selective hydrogenation of unsaturated aldehydes (acrolein, crotonaldehyde, and prenal) on platinum is an important reaction prototype[7] with a complex network of elementary steps. Indeed, four centers (three carbon and one oxygen) can be hydrogenated sequentially and with various orders. This reaction can competitively yield three possible partially hydrogenated products (unsaturated alcohol (UOL)—which is the target compound—saturated aldehyde (SAL), and the enol (ENOL)) and one completely hydrogenated saturated alcohol (SOL; see Schemes 1 and 2). Thus, a set of various carbon or oxygen reactive centers is obtained according to their position in the molecule, to the degree of hydrogenation of their neighboring atoms, or to the substitution by methyl groups for the terminal carbon C4. Finding a correlation between the chemical structure and the hydrogenation reactivity is a challenge.

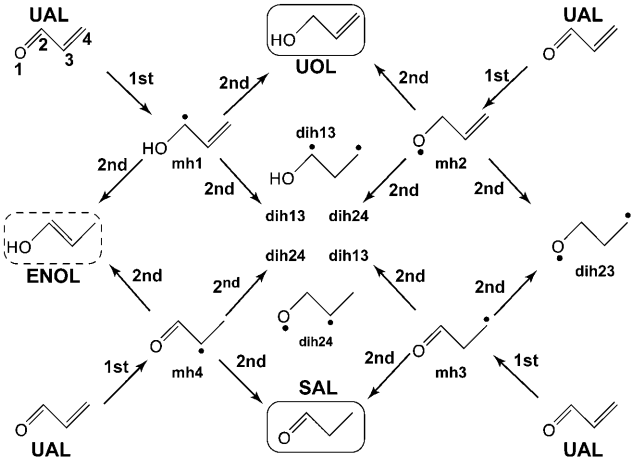

Scheme 1. First and second hydrogenation routes of *trans*-acrolein (UAL) on Pt(111) to yield monohydrogenated mh*i* and dihydrogenated dih*jk* species. Propen-2-ol (UOL) and propanal (SAL) are the competitive intermediate products.

In our recent studies, all the first and second hydrogenation routes of acrolein on Pt(111) were explored by DFT calculations. Smaller activation barriers were systematically obtained for the hydrogenation at the C=O bond. A preliminary microkinetic model based on the energy barriers calculated by DFT[8] showed a better selectivity for SAL on platinum, in agreement with experimental observations.[9] This selectivity results from a competition between the energy barriers of the surface hydrogenation steps and the desorption energies of the partially hydrogenated products. However, the picture remains incomplete in regard to the third and fourth hydrogenations that lead to SOL. Moreover, no explanation is offered to interpret the differences observed in the selectivity between acrolein and other unsaturated aldehydes, such as crotonaldehyde or prenal,[10] except desorption properties.[8]

In this study, we demonstrate by using an original definition of the Brønsted–Evans–Polanyi relation how the activation barriers of this prototype reaction can be predicted in a fast and accurate way. First, the linear scaling relations are illustrated for the hydrogenation pathways at the various sp^2

[*] Dr. D. Loffreda, Dr. F. Delbecq, Dr. F. Vigné, Dr. P. Sautet
Université de Lyon, CNRS, Laboratoire de Chimie
Ecole Normale Supérieure de Lyon
46 Allée d'Italie, 69364 Lyon Cedex 07 (France)
Fax: (+33) 4-7272-8860
E-mail: david.loffreda@ens-lyon.fr
Homepage: perso.ens-lyon.fr/david.loffreda

[**] We thank IDRIS at Orsay, CINES at Montpellier (project 609), and PSMN at Lyon for CPU time and assistance. We also acknowledge the ANR SIRE contract (ANR-06-CIS-014) and IDECAT network for financial support.

Supporting information for this article is available on the WWW under http://dx.doi.org/10.1002/anie.200902800.

centers of acrolein and its hydrogenated derivatives. They are then are validated with the hydrogenation of prenal and a few derivatives. Hence, we aim to demonstrate how the reactivity of these centers can be predicted from the calculation of only a few of them, thereby allowing the selectivity of a complete family of reactants to be determined or explained.

Only half of the complete reaction scheme was addressed in our previous investigation (see Scheme 1),[8] and we now complete the mechanistic picture in this study (Scheme 2; see the Supporting Information for all the details).

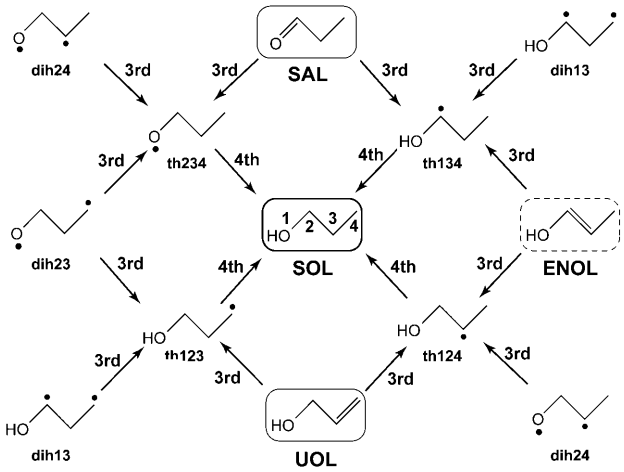

Scheme 2. Third and fourth hydrogenation routes of *trans*-acrolein derivatives on Pt(111) that yield the trihydrogenated species th*ijk* and the final product, the saturated alcohol (propanol, SOL).

A plot of the activation energy E_{act} against the reaction energy E_{hyd} of each of the 32 elementary steps involved in the complete hydrogenation mechanism of acrolein on Pt(111) (Figure 1a) does not show a linear relation. Hence, the classical BEP relation does not seem to apply. In contrast, a linear behavior is found (Figure 1b) when the energy of the transition state (E^{TS}_{coads}, or here also the activation energy E_{act}) is plotted against the energy of the precursor state (E^{IS}_{coads}). This coadsorption state formed between hydrogen and the reactant is the last stable or metastable structure just before the reaction occurs. The dispersion is large if the four reactive centers are considered together. However, the separation into three subsets (O1, C2, C3 + C4) gives a linear correlation of excellent quality (Table 1). For each subset the data points differ by the chemical environment of the reactive atoms. Notice that the slope of the line for the C2 subset is slightly different from that of the C3 and C4 centers. Hence, the BEP relation can be extended to the selective hydrogenation of acrolein on Pt(111), which proceeds by different formulation.

Table 1: Parameters of the linear relations between the coadsorption energies of the transition (TS) and of the initial (IS) states (separated reactants) for acrolein.[a]

$E^{TS}_{coads} = A \times E^{IS}_{coads} + B$	A	B	R^2
BEP at O1	1.0308	0.2785	0.9951
BEP at C2	0.8690	0.3391	0.9948
BEP at C3	1.0353	0.9034	0.9980
BEP at C4	1.0472	0.9149	0.9992

[a] See Figure 1c for definitions. R^2 = linear regression coefficient.

The good correlation obtained between the energy of the transition state and that of the precursor state originates from their geometrical similarity (hydrogen being adsorbed at a top site for attack at O1 and C2, or at hollow sites for attack at C2, C3, and C4, and the reactant adapting its adsorption structure). Our approach for hydrogenation agrees with previous relations, where the separated coadsorbed state corresponds conversely to the final state.[2,4,5] However, a variety of reactive centers in the molecule is explored here, instead of multiple catalytic surfaces.

The transferability of the exposed scaling relation[2] was then tested by considering another reactant. Prenal was selected because of the large difference in the selectivity observed on platinum. The results for the eight hydrogenation

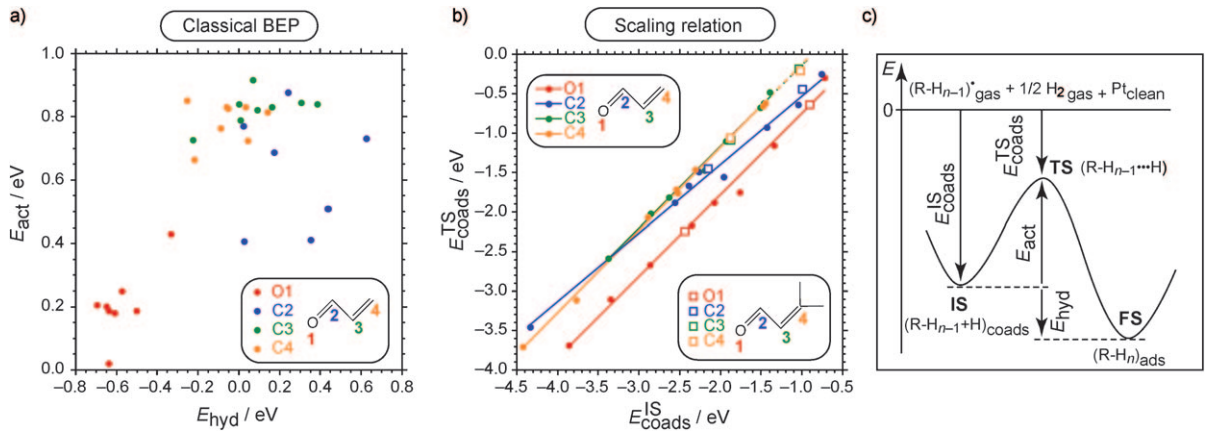

Figure 1. a) BEP diagram of the activation (E_{act}) versus the hydrogenation (E_{hyd}) energy for acrolein on Pt(111). b) Linear scaling relations (32 full circles) between the coadsorption energies of the transition (E^{TS}_{coads}) and the initial (E^{IS}_{coads}) states for acrolein on Pt(111) (see Table 1). The eight empty squares correspond to the first and some of the second hydrogenation steps of prenal on Pt(111). c) Definitions of the energies involved in the relations uncovered in (a) and (b); FS = final state.

Table 2: Applications of the linear relations demonstrated for acrolein (see Table 1) to some of the hydrogenation steps of prenal on the basis of the corresponding initial coadsorption states for prenal E_{coads}^{IS} [a].

$E_{act}^{corr} = (A-1) \times E_{coads}^{IS} + B$	$E_{coads\,s}^{IS}$	E_{act}^{corr}	E_{act}^{NEB}	ΔE[a]
TS^{h}_{1}	−0.91	0.25	0.27	−0.02
TS^{h}_{2}	−0.99	0.47	0.55	−0.08
TS^{h}_{3}	−1.04	0.87	0.86	0.01
TS^{h}_{4}	−1.02	0.87	0.81	0.06
TS^{h}_{12}	−2.15	0.62	0.70	−0.08
TS^{h}_{21}	−2.44	0.20	0.20	0.00
TS^{h}_{34}	−1.88	0.83	0.82	0.01
TS^{h}_{43}	−1.88	0.84	0.79	0.05

[a] ΔE is the error between the activation energy E_{act}^{corr} estimated by the correlations and those coming from the nudged elastic band (NEB) approach E_{act}^{NEB}. All the energies are in eV. h = hydrogenation.

steps optimized on Pt(111) are reported in Table 2 (see also the Supporting Information). In particular, the coadsorption energy of the initial precursor states E_{coads}^{IS} and the optimized activation barriers E_{act}^{NEB} are indicated. The corresponding eight points (2 points for each of the 4 sets) reported in Figure 1b (empty squares) fit perfectly with the correlations drawn for acrolein. Hence, the linear relations are validated for this second reactant. Thus, the corresponding activation barriers for the hydrogenation of prenal could have been estimated by applying the relations obtained for acrolein (E_{coads}^{IS} being the only data required to calculate E_{act}^{corr}, as shown in Table 2). The absolute error ΔE between the true energy barrier (E_{act}^{NEB}) and the estimated one (E_{act}^{corr}) ranges from 0 to 80 meV, which definitely shows the quality of the linear relations. More precisely, all the activation barriers for the hydrogenation of prenal on Pt(111) can be estimated very rapidly on the basis of only the geometry optimization of each initial precursor state. This model will have major consequences not only in answering the questions of the change in selectivity observed in the hydrogenation of crotonaldehyde and prenal on platinum, but presumably also in exploring many other reactions. Once the reactivity is known on a prototype process, it could simply be extended to a large range of molecular species by changing the environment of the reactive centers.

Hence, our density functional theory investigation of the complete hydrogenation pathways of acrolein and its partially hydrogenated derivatives on Pt(111) allows an extension of the Brønsted–Evans–Polanyi relation to be proposed. Linear relations between the transition-state and the precursor-state energies have been demonstrated for various pathways corresponding to hydrogen attack at a given reactive center of the molecule, whatever the chemical environment of the site. Our approach supports previous studies dealing with simple reactions of small molecules over transition-metal surfaces.

The scaling relations link the activation barriers of all the hydrogenation steps of the reactive centers and the adsorption energies of the corresponding precursor states. Their intrinsic quality is assigned to a chemical and structural analogy between the initial precursor state and the associated transition state.

The linear relations found allow the direct prediction of the differences in selectivity observed for other unsaturated aldehydes on platinum. In fact, they have been validated by examining the same reaction with prenal and its hydrogenated derivatives. More generally, it opens up promising perspectives for the quick examination of the reactivity of a whole family of organic compounds. By coupling these relations with others that change the chemical nature of the metal, our approach could provide a general tool for a fast and quantitative evaluation of the activity and selectivity of these catalysts. Moreover, other types of catalytic reactions could be examined with this model.

Experimental Section

The complete details of the methodology are reported in the Supporting Information. DFT calculations in periodic boundary conditions (VASP package[11]) were performed at the generalized gradient approximation with the Perdew Wang 91 exchange-correlation functional. Atomic cores were described with the projector-augmented-wave method. A cut-off of 400 eV was selected for the plane-wave basis-set expansion. A (3 × 3) supercell (four metal layers and a vacuum of 11.5 Å) on the Pt(111) surface was chosen with a (3 × 3 × 1) Monkhorst–Pack *k*-point mesh. The reaction pathways were minimized according to the climbing-image nudged elastic band (NEB) method.

Received: May 25, 2009
Revised: August 21, 2009
Published online: September 18, 2009

Keywords: density functional calculations · heterogeneous catalysis · hydrogenation · surface chemistry · unsaturated aldehydes

[1] a) J. N. Brønsted, *Chem. Rev.* **1928**, *5*, 231; b) M. G. Evans, M. Polanyi, *Trans. Faraday Soc.* **1938**, *34*, 11.
[2] a) J. K. Nørskov, T. Bligaard, A. Logadottir, S. Bahn, L. B. Hansen, M. Bollinger, H. Bengaard, B. Hammer, Z. Sljivancanin, M. Mavrikakis, Y. Xu, S. Dahl, C. J. H. Jacobsen, *J. Catal.* **2002**, *209*, 275; b) A. Logadottir, T. H. Rod, J. K. Nørskov, B. Hammer, S. Dahl, C. J. H. Jacobsen, *J. Catal.* **2001**, *197*, 229; c) F. Abild-Pedersen, J. Greeley, F. Studt, J. Rossmeisl, T. R. Munter, P. G. Moses, E. Skulason, T. Bligaard, J. K. Nørskov, *Phys. Rev. Lett.* **2007**, *99*, 016105.
[3] V. Pallassana, M. Neurock, *J. Catal.* **2000**, *191*, 301.
[4] R. A. van Santen, *Acc. Chem. Res.* **2009**, *42*, 57.
[5] D. Loffreda, F. Delbecq, D. Simon, P. Sautet, *J. Chem. Phys.* **2001**, *115*, 8101.
[6] A. Michaelides, Z.-P. Liu, C. J. Zhang, A. Alavi, D. A. King, P. Hu, *J. Am. Chem. Soc.* **2003**, *125*, 3704.
[7] P. Gallezot, D. Richard, *Catal. Rev. Sci. Eng.* **1998**, *40*, 81.
[8] D. Loffreda, F. Delbecq, F. Vigné, P. Sautet, *Angew. Chem.* **2005**, *117*, 5413; *Angew. Chem. Int. Ed.* **2005**, *44*, 5279; D. Loffreda, F. Delbecq, F. Vigné, P. Sautet, *J. Am. Chem. Soc.* **2006**, *128*, 1316.
[9] T. B. L. W. Marinelli, S. Nabuurs, V. Ponec, *J. Catal.* **1995**, *151*, 431; T. B. L. W. Marinelli, V. Ponec, *J. Catal.* **1995**, *156*, 51; V. Ponec, *Appl. Catal. A* **1997**, *149*, 27.
[10] P. Claus, *Top. Catal.* **1998**, *5*, 51; T. Birchem, C.-M . Pradier, Y. Berthier, G. Cordier, *J. Catal.* **1994**, *146*, 503; P. Beccat, J.-C. Bertolini, Y. Gauthier, J. Massardier, P. Ruiz, *J. Catal.* **1990**, *126*, 451.
[11] G. Kresse, J. Hafner, *Phys. Rev. B* **1993**, *47*, 558.

